Journal of Biomechanics 49 (2016) 2520–2530

Contents lists available at ScienceDirect

Journal of Biomechanics

journal homepage: www.elsevier.com/locate/jbiomech
www.JBiomech.com

Impact of different aortic valve calcification patterns on the outcome of transcatheter aortic valve implantation: A finite element study

Francesco Sturla [a,*], Mattia Ronzoni [a], Mattia Vitali [a], Annalisa Dimasi [a], Riccardo Vismara [a], Georgia Preston-Maher [b], Gaetano Burriesci [b], Emiliano Votta [a], Alberto Redaelli [a]

[a] Department of Electronics, Information and Bioengineering, Politecnico di Milano, Via Golgi 39, 20133 Milano, Italy
[b] UCL Cardiovascular Engineering Laboratory, UCL Mechanical Engineering, University College London, London, UK

ARTICLE INFO

Article history:
Accepted 19 March 2016

Keywords:
Aortic stenosis
Calcifications
TAVI
Biomechanics
Finite element models

ABSTRACT

Transcatheter aortic valve implantation (TAVI) can treat symptomatic patients with calcific aortic stenosis. However, the severity and distribution of the calcification of valve leaflets can impair the TAVI efficacy. Here we tackle this issue from a biomechanical standpoint, by finite element simulation of a widely adopted balloon-expandable TAVI in three models representing the aortic root with different scenarios of calcific aortic stenosis. We developed a modeling approach realistically accounting for aortic root pressurization and complex anatomy, detailed calcification patterns, and for the actual stent deployment through balloon-expansion.

Numerical results highlighted the dependency on the specific calcification pattern of the "dog–boning" of the stent. Also, local stent distortions were associated with leaflet calcifications, and led to localized gaps between the TAVI stent and the aortic tissues, with potential implications in terms of paravalvular leakage. High stresses were found on calcium deposits, which may be a risk factor for stroke; their magnitude and the extent of the affected regions substantially increased for the case of an "arc–shaped" calcification, running from commissure to commissure. Moreover, high stresses due to the interaction between the aortic wall and the leaflet calcifications were computed in the annular region, suggesting an increased risk for annular damage.

Our analyses suggest a relation between the alteration of the stresses in the native anatomical components and prosthetic implant with the presence and distribution of relevant calcifications. This alteration is dependent on the patient-specific features of the calcific aortic stenosis and may be a relevant indicator of suboptimal TAVI results.

1. Introduction

Transcatheter aortic valve implantation (TAVI) is a minimally invasive procedure currently used for the treatment of aortic stenosis (AS) in symptomatic patients with important contra-indications for surgery (Smith et al., 2011; Vahanian et al., 2008). TAVI consists in the percutaneous implantation of a biological heart valve mounted within a metal stent. The latter can be made from Ni–Ti super-elastic alloy, resulting in a self-expandable device, or from elasto-plastic metals (e.g. stainless steel, Co–Cr, etc.) in which case the prosthesis is balloon-expandable. In both cases, the stent expansion pushes the native aortic valve (AV) leaflets against the aortic root (AR). Correct stent expansion is essential to ensure that the device maintains its position after implantation, as well as a correct function of the prosthetic leaflets. TAVI candidates often present calcified aortic leaflets (Stewart et al., 1997) with variable and heterogeneous degrees and patterns of calcium deposits (Thubrikar et al., 1986), which may severely affect the expansion of the stent and, hence, *in vivo* implant outcomes (Detaint et al., 2009; Halevi et al., 2015; Rosenhek et al., 2000; Schievano et al., 2010). Possible complications include dislodgement or migration of the prosthetic device, paravalvular leakage and stroke, potentially associated to the breakdown of calcium deposits (Bax et al., 2014; Ewe et al., 2011; Webb and Wood, 2012). Given the key role of the mechanical interaction between the stent of the prosthetic device, the native AR and, in particular, the native AV, the mechanical analysis of TAVI function within a human AR affected by calcific AS is crucial to quantify and

Abbreviations: AR, aortic root; AS, aortic stenosis; AV, aortic valve; AVA, aortic valve area; CAS, calcific aortic stenosis; FE, finite element; R_C, commissural radial stent coordinate; R_{mid}, radial stent coordinate close to leaflets belly; TAVI, transcatheter aortic valve implantation; ε_r, radial strain; ε_θ, circumferential strain; σ_1, maximum principal stress; σ_{VM}, Von Mises stress

* Corresponding author. Tel.: +39 02 2399 3327.
E-mail address: francesco.sturla@polimi.it (F. Sturla).

http://dx.doi.org/10.1016/j.jbiomech.2016.03.036

understand the dependency of TAVI outcomes on calcifications severity and patterns.

In this perspective, numerical models represent a powerful tool, due to their inherent capability to analyze the sensitivity of a given system to different factors in a fully controlled and deterministic fashion, while accounting for complex geometry and material mechanical properties. This approach has been increasingly adopted to compute AR biomechanics following TAVI procedures. Anatomically detailed AR finite element (FE) models based on computed tomography have been used to predict the effects of different positioning (Capelli et al., 2012) and of focal calcifications (Wang et al., 2012) on the stent of a balloon-expandable TAVI device within a calcific AV, neglecting the presence of the prosthetic leaflets. More recently, both the implantation of balloon-expandable TAVI devices and the prosthesis diastolic biomechanics have been simulated (Auricchio et al., 2014; Morganti et al., 2014), although through the adoption of potentially relevant simplifying assumptions that may prevent from fully capturing the effects of the calcific disease in terms of stent and prosthetic leaflet distortions. These consisted either in neglecting: i) the presence of the native AV (Auricchio et al., 2014), ii) the presence of the balloon, thus forcing the expansion of the stent through a pre-defined and uniform radial displacement field independent of local increases in the stiffness of the surrounding anatomical structures (Morganti et al., 2014), or iii) the pressure loads acting on the AR wall (Morganti et al., 2014).

Also, different numerical studies have shown that the presence of AV leaflet calcifications can be considered, either through simplified approaches which assume leaflet stiffening (van Loon, 2010; Weinberg et al., 2009) or thickening (Dimasi et al., 2015; Katayama et al., 2013), or adopting more realistic models allowing for the detailed description of calcification locations and morphologies, based on *in vivo* imaging (Halevi et al., 2015; Morganti et al., 2014).

In this paper, we present a numerical study of the implantation of a clinically available and widely used balloon-expandable TAVI prosthesis within an anatomically realistic FE model of the human AR affected by calcific AS. The simulation combines the comprehensive descriptions of all of the steps of the TAVI procedure in a pressurized AR with realistic modeling of different AV calcification patterns, and with the simulation of the prosthesis function throughout the cardiac cycle. The aim of the study is to quantify the effects of different calcification patterns on TAVI outcome in terms of i) stent distortions, ii) prosthetic leaflets diastolic coaptation and systolic opening, iii) stent malposition with associated possible paravalvular leakage, iv) stress concentrations acting on calcifications during TAVI procedure, which may be indicative of increased risk of embolization of calcific material.

2. Materials and methods

A three-dimensional AR finite element model was implemented. Three different versions of the model were set, each one being characterized by a different pattern of AV leaflets calcification. For each version, the biomechanics of the AR associated to calcific AS was computed (named CAS simulations), the transapical TAVI procedure with an Edwards SAPIEN® device (Edward Lifesciences Inc.; Irvine, CA) was simulated, and the post-implant biomechanics of the prosthetic valve was estimated throughout a cardiac cycle (TAVI simulations). Simulations were run on the commercial FE explicit solver LS-DYNA© v. 971 (LSTC, Livermore, CA, USA) on an Intel Xeon (2.93 GHz) workstation with 12 processors.

2.1. AR geometry

The geometry of the AR model was identical to that previously described in Sturla et al., (2013), which accounts for the asymmetry of the three leaflet-sinus units, as well as for the curvature and tilting of the ascending aorta (Fig. 1a and b). The aortic wall, consisting of interleaflet triangles, Valsalva sinuses and ascending aorta, was modeled as a thick walled vessel with a homogeneous thickness of 2.3 mm (Grande et al., 1998), and discretized into linear hexahedral elements with reduced integration (characteristic dimension 0.2–0.4 mm). Dimensions and proportions of the aortic wall were defined averaging *in vivo* measurements from 10 healthy subjects, obtained through cardiac magnetic resonance imaging (Conti et al., 2010). AV leaflets were treated as thin structures and discretized into 4-node shell elements (characteristic dimension 0.2–0.4 mm), with geometry defined based on *ex vivo* data of leaflet surface dimensions and regional thickness variations (Fig. 1c) (Beller et al., 2004; Grande et al., 1998; Kunzelman et al., 1994). *In vivo* and *ex vivo* data were properly scaled to be all consistent with a 24 mm annular diameter (Labrosse et al., 2010).

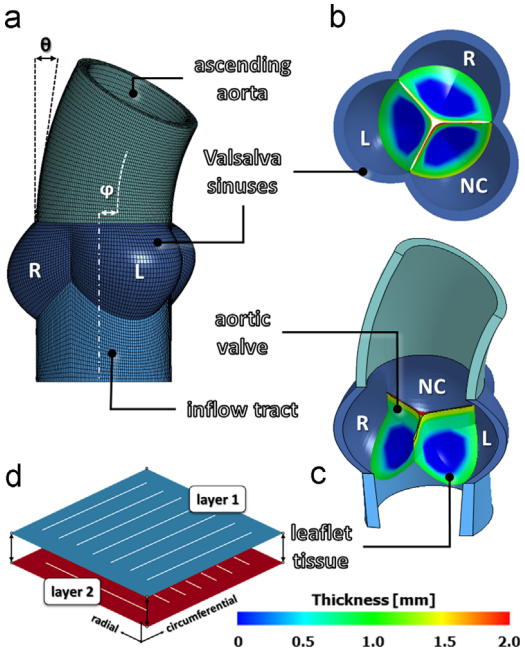

Fig. 1. Aortic root geometrical model as reproduced from Sturla et al. (2013): a–c) AR sub-structures, definition of the left (L), right (R) and non-coronary (NC) Valsalva sinuses, and redistribution of the local thickness on each AV leaflet; d) schematic representation of the two-layer FE model adopted to reproduce the macroscopic mechanical response of native AV leaflets, as proposed by Wenk et al. (2012).

2.2. AR tissues mechanical properties

AR wall tissue was assumed isotropic linear elastic, with a 2 MPa Young modulus and a 0.45 Poisson ratio (Sturla et al., 2013). The mechanical response of AV leaflets was modeled as hyperelastic, anisotropic and incompressible. In the real leaflet tissue, this macroscopic stress–strain behavior is the result of the tissue's microstructure, which is characterized by crimped collagen fibers preferentially aligned in the commissure–commissure direction, although with a degree of dispersion. In our model, we reproduced this macroscopic stress-strain behavior through the multilayer approach proposed by Wenk et al. (2012). Across the leaflet thickness, two layers of shell elements with shared nodes were defined (Fig. 1d), which accounted for 55% and 45% of the local leaflet thickness, respectively. The material of the two layers was described as fiber-reinforced, with the fibers oriented along the commissure-commissure and radial direction of the leaflet, respectively, through the invariant-based strain energy function proposed in Quapp and Weiss, (1998) and available in LS-DYNA:

$$W = \frac{C_1}{2}(\bar{I}_1 - 3) + \frac{C_2}{2}(\bar{I}_2 - 3) + F(\lambda) + \frac{1}{2}K\ln(J) \quad (1)$$

where W is the energy density function, $\bar{I}_1 = tr(C)$ and $\bar{I}_2 = \frac{1}{2}[tr(C)^2 - tr(C^2)]$ are the first and second invariant of the deviatoric component of the right Cauchy–Green strain tensor C, $J = det(F)$ is the determinant of the deformation gradient F, and K is the bulk modulus. $F(\lambda)$ represents the contribution of fibers along a defined fiber direction and satisfies the following conditions:

$$\lambda\frac{\partial F(\lambda)}{\partial \lambda} = \begin{cases} 0 & \lambda < 1 \\ C_3\left[e^{C_4(\lambda-1)} - 1\right] & 1 < \lambda < \lambda^* \\ C_5\lambda + C_6 & \lambda > \lambda^* \end{cases} \quad (2)$$

where λ is the stretch in the fiber direction, C_1–C_6 are material constants, and λ^* is the stretch value at which collagen fibers are straightened. As in Wenk et al. (2012), C_2 was set to 0, and the linear portion of the function (i.e. for $\lambda > \lambda^*$) was neglected